



HAL
open science

Adaptive Nonlinear Control of Induction Motors through AC/DC/AC Converters

Abderrahim Elfadili, Fouad Giri, Abdelmounime El Magri, Luc Dugard,
Fatima Zara Chaoui

► **To cite this version:**

Abderrahim Elfadili, Fouad Giri, Abdelmounime El Magri, Luc Dugard, Fatima Zara Chaoui. Adaptive Nonlinear Control of Induction Motors through AC/DC/AC Converters. Asian Journal of Control, 2012, 14 (6), pp.1470-1483. 10.1002/asjc.478 . hal-00638497

HAL Id: hal-00638497

<https://hal.science/hal-00638497>

Submitted on 7 Nov 2011

HAL is a multi-disciplinary open access archive for the deposit and dissemination of scientific research documents, whether they are published or not. The documents may come from teaching and research institutions in France or abroad, or from public or private research centers.

L'archive ouverte pluridisciplinaire **HAL**, est destinée au dépôt et à la diffusion de documents scientifiques de niveau recherche, publiés ou non, émanant des établissements d'enseignement et de recherche français ou étrangers, des laboratoires publics ou privés.

Adaptive Nonlinear Control of Induction Motors through AC/DC/AC Converters

A. El Fadili^{*1}, F. Giri¹, A. El Magri¹, L. Dugard², F.Z. Chaoui¹.

1. University of Caen Basse-Normandie, GREYC Lab UMR CNRS, 14032 Caen, France

2. GIPSA Lab UMR CNRS, Grenoble-INP, France

* Corresponding author: elfadili_abderrahim@yahoo.fr

Abstract. The problem of controlling induction motors, together with associated AC/DC rectifiers and DC/AC inverters, is addressed. The control objectives are threefold: (i) the motor speed should track any reference signal despite mechanical parameter **uncertainties** and **variations**; (ii) the DC Link voltage must be tightly regulated; (iii) **the** power factor correction (PFC) **w.r.t.** the power supply net must be performed in a satisfactory way. First, a nonlinear model of the whole controlled system is developed within the Park coordinates. Then, a multi-loop nonlinear adaptive controller is synthesized using the backstepping design technique. A formal analysis based on Lyapunov stability and average theory is **made to exhibit** the control system performances. In addition to closed-loop global asymptotic stability, it is proved that all control objectives (motor speed tracking, rotor flux regulation, DC link voltage regulation and unitary power factor) are asymptotically **achieved, up to small but unavoidable** harmonic errors (ripples).

Index Terms. Induction machines, speed and flux regulation, AC/DC/AC converters, PFC, Lyapunov methods, backstepping design technique.

1. INTRODUCTION

It is widely recognized that the induction motor has become a main actuator for industrial purposes. Indeed, as compared to the DC machine, it provides a better power/mass ratio, simpler maintenance (as it includes no mechanical commutators) and a relatively lower cost. However, the problem of controlling induction motors is more complex because these are multivariable and highly nonlinear **systems** and some of their parameters are time-varying. From the technological viewpoint, a considerable progress has been made in power electronics over the last two decades. Reliable power converters have become available which makes technically possible flexible speed variation of electrical drives including induction machines. Accordingly, **the** speed variation of these machines is **carried out** by acting on the supply **network** frequency. Similarly, before the recent progress in modern power electronics, there was no effective and flexible way to vary the frequency of a supply **network**. In this respect, recall that the power **networks** may be either DC or AC but mono-phase (this is for instance the case in the electric traction domain). Therefore, three-phase DC/AC inverters turn out to be the only possible interface (between railway **networks** and 3-phase AC motors) due to their high capability to ensure flexible voltage and frequency variation.

The control problem at hand is to design a speed controller for the complex system including an AC/DC rectifier, a DC/AC inverter and an induction motor. The controller is expected to ensure a wide range speed regulation, despite mechanical parameters' variations. Indeed, the rotor inertia moment, the viscous friction coefficient and the load torque are presently allowed to be unknown and step-like varying.

The rectifier is (of?) a pulse width modulation (PWM) type that features power regeneration, controlled DC-link voltage, small filter, 4-quadrant operation (bidirectional power transmission). Nowadays, the use of PWM rectifiers has considerably spread in industry and concerns a wide range spectrum of applications, [12], [4]. The point is that the association 'rectifier-inverter-motor' acts as a highly nonlinear load vis-à-vis to the main power AC network (which is supposed to provide almost perfect sinusoidal voltage to all other connected loads). Therefore, undesirable higher harmonics are generated (due to the load nonlinearity) and pollute the supply network. This harmonic pollution reduces the rectifier efficiency, induces voltage distortion in the AC supply network and induces electromagnetic compatibility problems [12].

In the light of the above considerations, it turns out that the control objective must not only be motor speed regulation but also the current harmonics rejection through power factor correction (PFC), [7]. In most previous works on induction machine speed control, the control problem was simplified by ignoring the dynamics of the AC/DC/AC converters. Accordingly, the machine is supposed to be directly controlled by stator voltages. The simplified control problem has been dealt with using several control strategies ranging from simple techniques, e.g. field-oriented control [5], to more sophisticated nonlinear approaches, e.g. passivity control [1], direct torque control [11], [3], or sliding mode control [10]. A control strategy that ignores the presence of the AC/DC rectifier suffers at least from two main drawbacks. First, the controller design relies on the assumption that the DC voltage (provided by the AC/DC rectifier) is perfectly regulated; the point is that perfect regulation of the rectifier output voltage cannot be ensured when ignoring the rectifier load which is nothing but the 'inverter-motor' set. The second drawback is concerned by the entire negligence of the PFC requirement. That is, from a control viewpoint, it is not judicious to consider separately the inverter-motor association, on one hand, and the power rectifier, on the other hand.

In the present work, we will develop a new control strategy that simultaneously accounts for all system components i.e. the AC/DC rectifier and the association 'DC/AC inverter-motor'. Our control strategy is featured by its multi-loops nature. First, a current loop is designed so that the coupling between the power supply network and the AC/DC rectifier operates with a unitary power factor. Then, a second loop is designed to regulate the output voltage of the AC/DC rectifier so that the DC-link between the rectifier and the inverter keeps on a constant voltage despite changes in the motor operation conditions. Finally, a bi-variable loop is designed to make the motor velocity track its

varying reference value and regulate the rotor flux norm to its nominal value. All control loops are designed using the Lyapunov and backstepping techniques [9]. Interestingly, the load torque, rotor inertia and friction coefficient are presently allowed to be unknown parameters subject to step-like changes. This parametric uncertainty is coped with, by providing the controller with a parameter adaptation capability. It will be formally proved that the proposed multi-loop nonlinear adaptive controller actually stabilizes (globally and asymptotically) the controlled system and meets its tracking objectives with a good accuracy. Specifically, the motor speed and rotor flux norm will be shown to perfectly track their references, whatever the initial conditions. The rectifier input current and output voltage are shown to match well their reference values. More precisely, the steady-state tracking errors for these two variables are both harmonic signals with amplitudes depending, among others, on the supply network frequency. These theoretical results are obtained by making a judicious use of adequate control theory tools, e.g. averaging theory and Lyapunov stability [8].

The paper is organized as follows: the system under study (i.e. the AC/DC/AC converter and induction motor association) is modeled and given a state space representation in Section 2; the controller design and the closed-loop system analysis are presented in Section 3; the controller performances are illustrated through numerical simulations in Section 4. For convenience, the main notations used throughout the paper are described in Table II given at the end of the paper.

2. MODELING ‘AC/DC/AC CONVERTER-INDUCTION MOTOR’ ASSOCIATION

The controlled system scheme is represented by Fig 1. It includes an AC/DC boost rectifier, on one hand, and an ‘inverter-induction motor’ combination, on the other hand. The inverter is a DC/AC converter operating, like the AC/DC rectifier, according to the known pulse width modulation (PWM) principle.

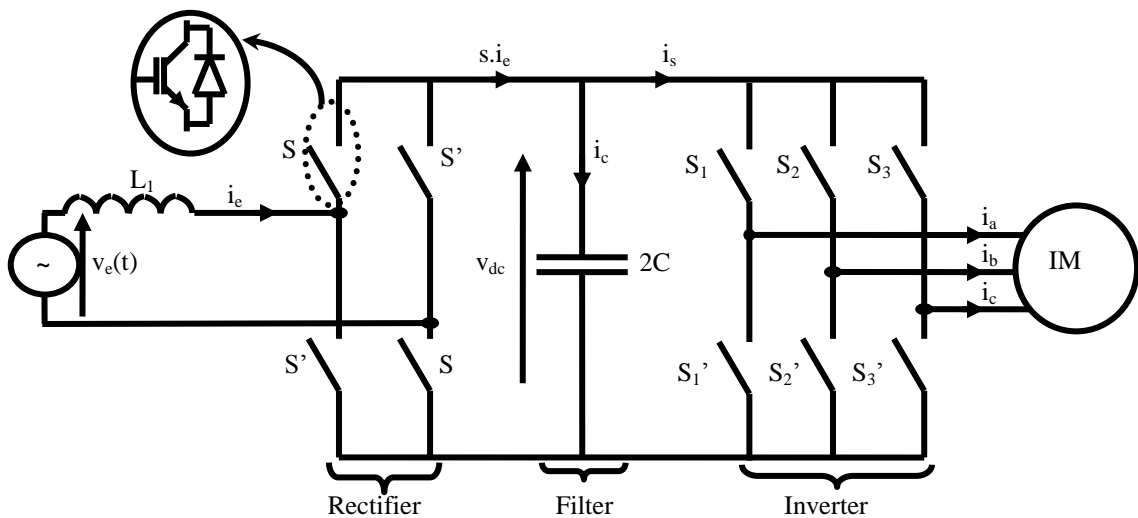


Fig.1. AC/DC/AC drive circuit with three-level inverter

2.1 AC/DC Rectifier Modeling

The power supply **network** is connected to an H-bridge **converter consisting** of four IGBT's with anti-parallel diodes for bidirectional power flow mode. The converter should be controlled so that two main tasks are accomplished: (i) providing a constant DC link voltage; (ii) ensuring an almost unitary power factor connection with the power **network**. Applying Kirchhoff's laws, this subsystem is described by the following set of differential equations:

$$\frac{di_e}{dt} = \frac{v_e}{L_1} - \frac{1}{L_1} s v_{dc} \quad (1a)$$

$$\frac{dv_{dc}}{dt} = \frac{1}{2C} s i_e - \frac{1}{2C} i_s \quad (1b)$$

where i_e is the current in inductor L_1 , v_{dc} denotes the voltage in capacitor $2C$, i_s designates the input current inverter, $v_e = \sqrt{2}.E.\cos(\omega_e t)$ is the sinusoidal **network** voltage (with known constants E, ω_e) and s is the switch position function taking values in the discrete set $\{-1, 1\}$. Specifically:

$$s = \begin{cases} 1 & \text{if } S \text{ is ON and } S' \text{ is OFF} \\ -1 & \text{if } S \text{ is OFF and } S' \text{ is ON} \end{cases} \quad (1c)$$

The above (instantaneous) model describes accurately the physical inverter. Then, it is based upon to build up converter simulators. However, it is not suitable for control design due to the switched nature of the control input s . As a matter of fact, most existing nonlinear control approaches apply to systems with continuous control inputs. Therefore, **the control** design for the above converter will be performed using the following average version of (1a-b) [6]:

$$\frac{dx_1}{dt} = \frac{v_e}{L_1} - \frac{1}{L_1} u_1 x_2 \quad (2a)$$

$$\frac{dx_2}{dt} = \frac{1}{2C} u_1 x_1 - \frac{1}{2C} \bar{i}_s \quad (2b)$$

where:

$$x_1 = \bar{i}_e, \quad x_2 = \bar{v}_{dc}, \quad u_1 = \bar{s} \quad (2c)$$

are the average values **over the** cutting periods of i_e , v_{dc} and s , respectively.

2.2 Inverter-Motor Modeling

The induction model is based on the motor equations in **the** rotating α -and- β axes and reads as:

$$\frac{d\Omega}{dt} = -\frac{f}{J}\Omega + \frac{m}{J}(i_{s\beta}\phi_{r\alpha} - i_{s\alpha}\phi_{r\beta}) - \frac{T_L}{J} \quad (3a)$$

$$\frac{di_{s\alpha}}{dt} = ba\phi_{r\alpha} + bp\Omega\phi_{r\beta} - \gamma i_{s\alpha} + m_1 v_{s\alpha} \quad (3b)$$

$$\frac{di_{s\beta}}{dt} = ba\phi_{r\beta} - bp\Omega\phi_{r\alpha} - \gamma i_{s\beta} + m_1 v_{s\beta} \quad (3c)$$

$$\frac{d\phi_{r\alpha}}{dt} = -a\phi_{r\alpha} + aM_{sr}i_{s\alpha} - p\Omega\phi_{r\beta} \quad (3d)$$

$$\frac{d\phi_{r\beta}}{dt} = -a\phi_{r\beta} + aM_{sr}i_{s\beta} + p\Omega\phi_{r\alpha} \quad (3e)$$

where $i_{s\alpha}, i_{s\beta}, \phi_{r\alpha}, \phi_{r\beta}, \Omega$, and, T_L , are the stator currents, rotor fluxes, angular speed, and load torque, respectively. Wherever they come in, the subscripts s and r refer to the stator and rotor, respectively. That is, R_s and R_r are the stator and rotor resistances; L_s and L_r are the self-inductances. M_{sr} denotes the mutual inductance between the stator and rotor windings. p designates the number of pole-pairs, J the inertia of the motor-load set, and f is the friction coefficient. The remaining parameters are defined as follows:

$$a = \frac{R_r}{L_r}, \quad b = \frac{M_{sr}}{\sigma L_s L_r}, \quad \gamma = (L_r^2 R_s + M_{sr}^2 R_r) / \sigma L_s L_r^2, \quad \sigma = 1 - (M_{sr}^2 / L_s L_r), \quad m = p \frac{M_{sr}}{L_r}, \quad m_1 = \frac{1}{\sigma L_s}.$$

In (3a-e), $v_{s\alpha}, v_{s\beta}$ are the stator voltage in the $\alpha\beta$ -coordinates (Park's transformation of the three phase stator voltages). The inverter is featured by the fact that the stator α - and β -voltages can be controlled independently. To this end, these voltages are expressed in function of the corresponding control action (see e.g. [2]):

$$v_{s\beta} = v_{dc} u_3, \quad v_{s\alpha} = v_{dc} u_2 \quad (4a)$$

where (u_2, u_3) represent the average α - and β -axes (Park's transformation) of the three phase duty ratio system (s_1, s_2, s_3) . The latter are defined by (1c) replacing there (S, S') by (S_i, S'_i) ($i = 1, 2, 3$).

Now, let us introduce the state variables:

$$x_3 = \bar{\Omega}, \quad x_4 = \bar{i}_{s\alpha}, \quad x_5 = \bar{i}_{s\beta}, \quad x_6 = \bar{\phi}_{r\alpha}, \quad x_7 = \bar{\phi}_{r\beta}, \quad (4b)$$

where the bar refers to signal averaging over cutting periods (just as in (2c)). Using the power conservation principle, the power absorbed by the DC/AC inverter is given by the usual expression

$P_{ai} = x_2 \bar{i}_s$. On the other hand, the power released by the inverter is given by $P_{rm} = x_2(u_2 x_4 + u_3 x_5)$. As

$P_{ai} = P_{rm}$, it follows that:

$$\bar{i}_s = (u_2 x_4 + u_3 x_5) \quad (4c)$$

Then, substituting (4a-c) in (3a-e) yields the following state-space representation of the association 'inverter-motor':

$$\frac{dx_3}{dt} = -\frac{f}{J} x_3 + \frac{m}{J} (x_5 x_6 - x_7 x_4) - \frac{T_L}{J} \quad (5a)$$

$$\frac{dx_4}{dt} = bax_6 + bpx_3x_7 - \gamma x_4 + m_1u_2x_2 \quad (5b)$$

$$\frac{dx_5}{dt} = bax_7 - bpx_3x_6 - \gamma x_5 + m_1u_3x_2 \quad (5c)$$

$$\frac{dx_6}{dt} = -ax_6 + aM_{sr}x_4 - px_3x_7 \quad (5d)$$

$$\frac{dx_7}{dt} = -ax_7 + aM_{sr}x_5 + px_3x_6 \quad (5e)$$

The state space equations **thus obtained** are put together to get a state-space model of the whole system including the AC/DC/AC converters and the induction motor. For convenience, the whole **system's** model is rewritten here for future reference:

$$\frac{dx_1}{dt} = \frac{v_e}{L_1} - \frac{1}{L_1}u_1x_2 \quad (6a)$$

$$\frac{dx_2}{dt} = \frac{1}{2C}u_1x_1 - \frac{1}{2C}(u_2x_4 + u_3x_5) \quad (6b)$$

$$\frac{dx_3}{dt} = -\frac{f}{J}x_3 + \frac{m}{J}(x_5x_6 - x_7x_4) - \frac{T_L}{J} \quad (6c)$$

$$\frac{dx_4}{dt} = bax_6 + bpx_3x_7 - \gamma x_4 + m_1u_2x_2 \quad (6d)$$

$$\frac{dx_5}{dt} = bax_7 - bpx_3x_6 - \gamma x_5 + m_1u_3x_2 \quad (6e)$$

$$\frac{dx_6}{dt} = -ax_6 + aM_{sr}x_4 - px_3x_7 \quad (6f)$$

$$\frac{dx_7}{dt} = -ax_7 + aM_{sr}x_5 + px_3x_6 \quad (6g)$$

3. CONTROLLER DESIGN

3.1 Control Objectives

There are two operational control objectives:

(i) Speed regulation: the machine speed Ω must track, as closely as possible, a given reference signal Ω_{ref} , despite the parametric **uncertainties** (concerning the load torque T_L , rotor inertia J and friction coefficient f).

(ii) PFC requirement: the rectifier input current i_e must be sinusoidal and in phase or opposed phase with the AC supply voltage v_e .

As there are three control inputs at hand, namely u_1 , u_2 and u_3 , two more control objectives are added:

(iii) Controlling the continuous voltage v_{dc} making it track a given reference signal v_{dcref} .

(iv) Regulating the rotor flux norm $\Phi_r = \sqrt{x_6^2 + x_7^2}$ to a reference value Φ_{ref} , preferably equal to its nominal value.

3.2 AC/DC rectifier control design

3.2.1 Controlling rectifier input current to meet PFC

The PFC objective means that the input current rectifier should be sinusoidal and in phase (or opposite phase) with the AC supply voltage. Therefore, one seeks a regulator that enforces the current x_1 to track a reference signal x_1^* of the form:

$$x_1^* = k v_e \quad (7)$$

At this point, k is any real parameter that is allowed to be time-varying. This parameter is positive when the induction machine operates in motor mode **and negative in the** generator mode. Introduce the current tracking error:

$$z_1 = x_1 - x_1^* \quad (8)$$

In view of (6a), the above error undergoes the following equation:

$$\dot{z}_1 = v_e / L_1 - u_1 x_2 / L_1 - \dot{x}_1^* \quad (9)$$

To get a stabilizing control law for this first-order system, consider the quadratic Lyapunov function $V_1 = 0.5 z_1^2$. It can be easily checked that the time-derivative \dot{V}_1 is a negative definite function of z_1 if the control input is chosen as follows:

$$u_1 = L_1 (c_1 z_1 + (v_e / L_1) - \dot{x}_1^*) / x_2 \quad (10)$$

with $c_1 > 0$ is a design parameter. The properties of **such a control** law are summarized in the following proposition, the proof of which is straightforward.

Proposition 1. *Consider the system, next called current (or inner) loop, composed of the current equation (6a) and the control law (10) where $c_1 > 0$ is arbitrarily chosen by the user. If the reference $x_1^* = k v_e$ and its first time derivative are **available**, then one has the following properties:*

1) *The current loop undergoes the equation $\dot{z}_1 = -c_1 z_1$ with $z_1 = x_1 - x_1^*$. As c_1 is **positive**, this equation is globally exponentially **stable**, i.e. z_1 vanishes exponentially, whatever the initial conditions.*

2) If in addition k converges (to a finite value), then the PFC requirement is asymptotically fulfilled in average i.e. the (average) input current x_1 tends (exponentially fast) to its reference $k v_e$ as $t \rightarrow \infty$ \square

3.2.2 DC link voltage regulation

The aim is now to design a tuning law for the ratio k in (7) so that the rectifier output voltage $x_2 = \bar{v}_{dc}$ is steered to a given reference value v_{dcref} . As mentioned above, v_{dcref} is generally (but not mandatory) set to the nominal value of the stator voltage amplitude. The first step in designing such a tuning law is to establish the relation between the ratio k (control input) and the output voltage x_2 . This is the subject of the following proposition.

Proposition 2. Consider the power rectifier described by (6a-b) together with the control law (10). Under the same assumptions as in Proposition 1, one has the following properties:

1) The output voltage x_2 varies, in response to the tuning ratio k , according to the equation:

$$\frac{dx_2}{dt} = \frac{1}{2C x_2} (k v_e^2 + z_1 v_e) - \frac{1}{2C} (u_2 x_4 + u_3 x_5) \quad (11)$$

2) The squared voltage ($y = x_2^2$) varies, in response to the tuning ratio k , according to the equation:

$$\frac{dy}{dt} = k v_e^2 / C + z_1 v_e / C + \chi(x, t) \quad (12)$$

with

$$\chi(x, t) = -x_2 (u_2 x_4 + u_3 x_5) / C \quad (13) \square$$

Proof. The power absorbed by the AC/DC rectifier is given by the well known expression $P_{absorbed} = x_1 v_e$. On the other hand, the power released by the rectifier (toward the load including the capacity and the inverter) is given by $P_{released} = u_1 x_1 x_2$. Using the power conservation principle, one has $P_{absorbed} = P_{released}$ or, equivalently:

$$x_1 v_e = u_1 x_1 x_2 \quad (14)$$

Also, from (7)-(8), one immediately gets that $x_1 = k v_e + z_1$ which together with (14) yields $u_1 x_1 = (k v_e^2 + z_1 v_e) / x_2$. This establishes (11) due to (6b). Deriving $y = x_2^2$ with respect to time and using (11) yields relation (12) and completes the proof of Proposition 2 \blacksquare

The ratio k stands up as a control signal in the first-order system defined by (12). As previously mentioned, the reference signal $y_{ref} \stackrel{def}{=} v_{dcref}^2$ (of the squared DC-link voltage $x_2 = v_{dc}$) is chosen to be constant (i.e. $\dot{y}_{ref} = 0$), it is given the nominal value of stator voltage amplitude. Then, it follows from (12) that the tracking error $z_2 = y - y_{ref}$ undergoes the following equation:

$$\dot{z}_2 = E^2 k / C + E^2 k \cos(2\omega_e t) / C + \sqrt{2} E z_1 \cos(\omega_e t) / C + \chi(x, t) - \dot{y}_{ref} \quad (15)$$

where **one used** the fact that $v_e = \sqrt{2} \cdot E \cdot \cos(\omega_e t)$ and $v_e^2 = E^2 (1 + \cos(2\omega_e t))$. To get a stabilizing control law for the system (15), consider the following quadratic Lyapunov function:

$$V_2 = 0.5 z_2^2 \quad (16)$$

It is easily checked that the time-derivative \dot{V}_2 can be made negative definite in the state z_2 by letting:

$$k E^2 + k E^2 \cos(2\omega_e t) + \sqrt{2} E z_1 \cos(\omega_e t) = C (-c_2 z_2 - \chi(x, t)) + C \dot{y}_{ref} \quad (17a)$$

where $c_2 > 0$ is a design parameter. The point is that **such an equation** involves a periodic singularity due to the mutual neutralization of the first two terms on the left side of (17a). To get off this singularity and, besides, to avoid an excessive chattering in the solution, the two terms in $\cos(\cdot)$ on the left side of (17a) are **ignored, leading** to the following approximate simpler solution:

$$k = C (-c_2 z_2 - \chi(x, t)) / E^2 + C \dot{y}_{ref} / E^2 \quad (17b)$$

Bearing in mind the fact that the first derivative of the control ratio k must be available (Proposition 1), the following filtered version of the above solution is proposed:

$$\dot{k} + d k = d C (-c_2 z_2 - \chi(x, t)) / E^2 + d C \dot{y}_{ref} / E^2 \quad (18)$$

At this point, the regulator parameters (d, c_2) are any positive real constants. The proof of the forthcoming proposition 3 (?) will make it clear how these should be chosen for the control objectives to be achieved. For now, let us summarize the main **findings (?)** in the following proposition.

Proposition 3. *Consider the inner control loop consisting of the AC/DC rectifier described by (6a-b) together with the control laws (10) and (18). Using Proposition 1 (Part 1), it turns out that the inner loop undergoes, in the (z_1, z_2, k) -coordinates, the following equation, where $z_1 = x_1 - x_1^*$ and $z_2 = y - y_{ref}$:*

$$\begin{pmatrix} \dot{z}_1 \\ \dot{z}_2 \\ \dot{k} \end{pmatrix} = \begin{pmatrix} -c_1 & 0 & 0 \\ 0 & 0 & \frac{E^2}{C} \\ 0 & -\frac{d C}{E^2} c_2 & -d \end{pmatrix} \begin{pmatrix} z_1 \\ z_2 \\ k \end{pmatrix} + \begin{pmatrix} 0 \\ 1 \\ -\frac{d C}{E^2} \end{pmatrix} (\chi(x, t) - \dot{y}_{ref}) + \begin{pmatrix} 0 \\ \frac{E^2}{C} k \cos(2\omega_e t) + \frac{\sqrt{2}}{C} E z_1 \cos(\omega_e t) \\ 0 \end{pmatrix} \quad (19) \quad \square$$

3.3 Motor speed and rotor flux norm regulation

The problem of controlling the rotor speed and flux norm is **now** addressed for the induction machine described by (5a-e). The speed reference Ω_{ref} is any bounded and derivable function of time and its two first derivatives are available and bounded. These properties can always be achieved filtering the reference through second-order linear filters. The flux reference Φ_{ref} is fixed to its nominal value. The controller design will now be performed in two steps using the tuning-functions backstepping adaptive technique [9]. First, introduce the tracking errors:

$$z_3 = \Omega_{ref} - x_3 \quad (20)$$

$$z_4 = \Phi_{ref}^2 - (x_6^2 + x_7^2) \quad (21)$$

Step 1. It follows from (5a) and (5d-e) that the errors z_3 and z_4 undergo the differential equations:

$$\dot{z}_3 = \dot{\Omega}_{ref} - m(x_6x_5 - x_7x_4) / J + T_L / J + f x_3 / J \quad (22)$$

$$\dot{z}_4 = 2\Phi_{ref} \dot{\Phi}_{ref} - 2aM_{sr}(x_6x_4 + x_7x_5) + 2a(\Phi_{ref}^2 - z_4) \quad (23)$$

In (22) and (23), the quantities $m(x_6x_5 - x_7x_4)$ and $2aM_{sr}(x_6x_4 + x_7x_5)$ stand up as virtual control signals. If these were the actual control signals, the error system (22)-(23) could be globally asymptotically **stabilized by letting** $m(x_6x_5 - x_7x_4) = \mu_1$ and $2aM_{sr}(x_6x_4 + x_7x_5) = \nu_1$ with:

$$\mu_1 \stackrel{def}{=} J(c_3 z_3 + \dot{\Omega}_{ref}) + T_L + f(\Omega_{ref} - z_3) \quad (24a)$$

On the other hand, the fact J , T_L and f are unknown suggests the certainty equivalence from of equations (24a).

$$\mu_1 = \hat{J}(c_3 z_3 + \dot{\Omega}_{ref}) + \hat{T}_L + \hat{f}(\Omega_{ref} - z_3) \quad (24b)$$

$$\nu_1 \stackrel{def}{=} c_4 z_4 + 2\Phi_{ref} \dot{\Phi}_{ref} + 2a(\Phi_{ref}^2 - z_4) \quad (25)$$

where c_3 and c_4 are any positive design parameters and \hat{J} , \hat{T}_L and \hat{f} are the estimates of J , T_L and f respectively. Indeed, considering the Lyapunov function:

$$V_3 = 0.5(z_3^2 + z_4^2) \quad (26)$$

one would get from (22)-(23), letting $m(x_6x_5 - x_7x_4) = \mu_1$ and $2aM_{sr}(x_6x_4 + x_7x_5) = \nu_1$:

$$\dot{V}_3 = -c_3 z_3^2 - c_4 z_4^2 \quad (27)$$

This would prove the global asymptotic stability of the system (22)-(25). As the quantities $m(x_6x_5 - x_7x_4)$ and $2aM_{sr}(x_6x_4 + x_7x_5)$ are not the actual control signals, they cannot be let equal to μ_1

and v_1 , respectively. Nevertheless, we retain the expressions of μ_1 and v_1 as first stabilizing functions and introduce the new errors:

$$z_5 = \mu_1 - m(x_6x_5 - x_7x_4) \quad (28)$$

$$z_6 = v_1 - 2aM_{sr}(x_6x_4 + x_7x_5) \quad (29)$$

Then, using the notations (24) to (29), the dynamics of the errors z_3 and z_4 , initially described by (22)-(23), can be rewritten as follows:

$$\dot{z}_3 = -c_3z_3 + \tilde{J}(c_3z_3 + \dot{\Omega}_{ref})/J + \tilde{T}_L/J + \tilde{f}x_3/J + z_5/J \quad (30)$$

$$\dot{z}_4 = -c_4z_4 + z_6 \quad (31)$$

where

$$\tilde{J} = J - \hat{J}, \quad \tilde{T}_L = T_L - \hat{T}_L \quad \text{and} \quad \tilde{f} = f - \hat{f} \quad (32)$$

Step 2. The second design step consists in choosing the actual control signals, u_2 and u_3 , so that all errors (z_3, z_4, z_5, z_6) converge to zero. To this end, we should **make (?)** how these errors depend on the actual control signals (u_2, u_3). We start focusing on z_5 ; it follows from (28) that:

$$\dot{z}_5 = \dot{\mu}_1 - m(\dot{x}_6x_5 + x_6\dot{x}_5 - \dot{x}_7x_4 - x_7\dot{x}_4) \quad (33)$$

Assume that the parameters J , T_L and f are **constant** or slowly time-varying and using (5a-e), (32) and (24), one gets from (33):

$$\begin{aligned} \dot{z}_5 = & \mu_2 + (c_3\hat{J} - \hat{f})z_5/J + mm_1x_2(x_7u_2 - x_6u_3) \\ & + (c_3\hat{J} - \hat{f}) \left[\frac{\tilde{J}}{J}(c_3z_3 + \dot{\Omega}_{ref}) + \frac{\tilde{T}_L}{J} + \frac{\tilde{f}}{J}x_3 \right] - \left[\tilde{J}(c_3z_3 + \dot{\Omega}_{ref}) + \tilde{T}_L + \tilde{f}x_3 \right] \end{aligned} \quad (34)$$

with

$$\begin{aligned} \mu_2 = & \left[-c_3z_3(c_3\hat{J} - \hat{f}) + \hat{J}\ddot{\Omega}_{ref} + \hat{f}\dot{\Omega}_{ref} \right] + m(a + \gamma)(x_6x_5 - x_7x_4) \\ & + mp_x(x_7x_5 + x_6x_4) + mbp_x(x_6^2 + x_7^2) \end{aligned} \quad (35)$$

Similarly, it follows from (29) that z_6 undergoes the following differential equation:

$$\dot{z}_6 = \dot{v}_1 - 2aM_{sr}(\dot{x}_6x_4 + x_6\dot{x}_4 + \dot{x}_7x_5 + x_7\dot{x}_5) \quad (36)$$

Using (5a-e) and (25), it follows from (36):

$$\dot{z}_6 = v_2 - 2aM_{sr}m_1(x_6u_2 + x_7u_3) \quad (37)$$

with

$$\begin{aligned} v_2 = & (c_4 - 2a)(-c_4 z_4 + z_6) + 2\Phi_{ref} \ddot{\Phi}_{ref} + 2\dot{\Phi}_{ref}^2 + 4a\Phi_{ref} \dot{\Phi}_{ref} + 2aM_{sr} p x_3 (x_7 x_4 - x_5 x_6) \\ & + 2aM_{sr} (a + \gamma)(x_4 x_6 + x_5 x_7) - 2(aM_{sr})^2 (x_4^2 + x_5^2) - 2a^2 b M_{sr} (\Phi_{ref}^2 - z_4) \end{aligned} \quad (38)$$

To analyze the error system, composed of equations (30-31), (34) and (37-38), let us consider the following augmented Lyapunov function candidate:

$$V_4 = 0.5 z_3^2 + 0.5 z_4^2 + 0.5 z_5^2 + 0.5 z_6^2 + 0.5 \tilde{J}^2 / J + 0.5 \tilde{T}_L^2 / J + 0.5 \tilde{f}^2 / J \quad (39)$$

Its time-derivative along the trajectory of the state vector (z_3, z_4, z_5, z_6) is:

$$\dot{V}_4 = z_3 \dot{z}_3 + z_4 \dot{z}_4 + z_5 \dot{z}_5 + z_6 \dot{z}_6 + \tilde{J} \dot{\tilde{J}} / J + \tilde{f} \dot{\tilde{f}} / J + \tilde{T}_L \dot{\tilde{T}}_L / J \quad (40)$$

Using (30), (34) and (37) in (40) and adding $c_5 z_5^2 - c_5 z_5^2 + c_6 z_6^2 - c_6 z_6^2$ yields:

$$\begin{aligned} \dot{V}_4 = & -c_3 z_3^2 - c_4 z_4^2 - c_5 z_5^2 - c_6 z_6^2 - f z_5^2 / J + z_3 z_5 / J \\ & + \frac{\tilde{J}}{J} \left[\dot{\tilde{J}} + (c_3 z_3 + \dot{\Omega}_{ref}) z_3 + z_5 (c_3 \hat{J} - \hat{f}) (c_3 z_3 + \dot{\Omega}_{ref}) - c_3 z_5^2 \right] + \frac{\tilde{T}_L}{J} \left[\dot{\tilde{T}}_L + z_3 + z_5 (c_3 \hat{J} - \hat{f}) \right] \\ & + \frac{\tilde{f}}{J} \left[\dot{\tilde{f}} + z_3 x_3 + z_5 x_3 (c_3 \hat{J} - \hat{f}) + z_5^2 \right] + z_6 [c_6 z_6 + z_4 + v_2 - 2aM_{sr} x_2 m_1 (x_6 u_2 + x_7 u_3)] \\ & + z_5 \left[\mu_2 + (c_5 + c_3) z_5 + m_1 x_2 (x_7 u_2 - x_6 u_3) - \left[\tilde{J} (c_3 z_3 + \dot{\Omega}_{ref}) + \tilde{T}_L + \tilde{f} x_3 \right] \right] \end{aligned} \quad (41)$$

This suggests the following parameter adaptation laws :

$$\dot{\tilde{T}}_L = -\lambda_{T_L} \tilde{T}_L, \quad \dot{\tilde{J}} = -\lambda_J \tilde{J} \quad \text{and} \quad \dot{\tilde{f}} = -\lambda_f \tilde{f} \quad (42)$$

erehw

$$\lambda_J = -c_3 z_5^2 + z_3 (c_3 z_3 + \dot{\Omega}_{ref}) + z_5 (c_3 \hat{J} - \hat{f}) (c_3 z_3 + \dot{\Omega}_{ref}) \quad (43a)$$

$$\lambda_{T_L} = z_3 + (c_3 \hat{J} - \hat{f}) z_5 \quad (43b)$$

$$\lambda_f = z_3 x_3 + z_5 x_3 (c_3 \hat{J} - \hat{f}) + z_5^2 \quad (43c)$$

from (32) and (42), the expressions of \hat{J} , \hat{T}_L and \hat{f} can be calculated with the following equations:

$$\dot{\hat{J}} = \lambda_J, \quad \dot{\hat{T}}_L = \lambda_{T_L}, \quad \dot{\hat{f}} = \lambda_f \quad (44)$$

Substituting the parameter adaptation laws (42) to \tilde{T}_L , \tilde{J} and \tilde{f} in the right side of (41) yields:

$$\begin{aligned} \dot{V}_4 = & -c_3 z_3^2 - c_4 z_4^2 - c_5 z_5^2 - c_6 z_6^2 - \frac{f}{J} z_5^2 + \frac{1}{J} z_3 z_5 + z_6 [v_2 + z_4 + c_6 z_6 - 2aM_{sr} x_2 m_1 (x_6 u_2 + x_7 u_3)] \\ & + z_5 \left[\mu_2 + (c_5 + c_3) z_5 + m_1 x_2 (x_7 u_2 - x_6 u_3) + \left[\lambda_J (c_3 z_3 + \dot{\Omega}_{ref}) + \lambda_{T_L} + \lambda_f x_3 \right] \right] \end{aligned} \quad (45)$$

where c_5 and c_6 are new positive real design parameters. Equation (45) suggests that the control signals u_2, u_3 must be chosen so that the two quantities between curly brackets (on the right side of (45)) are set to zero. Letting these quantities equal to zero and solving the resulting second-order linear equation system with respect to (u_2, u_3) , gives the following control law:

$$\begin{bmatrix} u_2 \\ u_3 \end{bmatrix} = \begin{bmatrix} \lambda_0 & \lambda_1 \\ \lambda_2 & \lambda_3 \end{bmatrix}^{-1} \begin{bmatrix} -[\lambda_J(c_3 z_3 + \dot{\Omega}_{ref}) + \lambda_{T_L} + \lambda_f x_3] - (c_5 + c_3)z_5 - \mu_2 \\ -z_4 - c_6 z_6 - v_2 \end{bmatrix} \quad (46)$$

with:

$$\lambda_0 = m_1 x_7 x_2, \quad \lambda_1 = -m_1 x_6 x_2, \quad \lambda_2 = -2aM_{sr} x_6 x_2, \quad \lambda_3 = -2aM_{sr} x_7 x_2 \quad (47)$$

It is worth noting that the matrix $\begin{bmatrix} \lambda_0 & \lambda_1 \\ \lambda_2 & \lambda_3 \end{bmatrix}$ is nonsingular. Indeed, it is easily checked that its

determinant is $D = \lambda_0 \lambda_3 - \lambda_1 \lambda_2 = -2m_1 a M_{sr} x_2^2 (x_6^2 + x_7^2)$ **never vanishes** in practice because of the machine remnant flux. Substituting the control law (46) to (u_2, u_3) on the right side of (45) yields:

$$\dot{V}_4 = -c_3 z_3^2 - c_4 z_4^2 - c_5 z_5^2 - c_6 z_6^2 - f z_5^2 / J + z_3 z_5 / J \quad (48a)$$

By using the following inequality:

$$\sqrt{|z_3|} \sqrt{|z_5|} \leq \frac{\theta}{2} z_3^2 + \frac{1}{2\theta} z_5^2 \quad (48b)$$

$\forall \theta \in]0,1[$ **we obtain:**

$$\dot{V}_4 \leq -\vartheta_3 z_3^2 - c_4 z_4^2 - \vartheta_5 z_5^2 - c_6 z_6^2 \quad (49)$$

where

$$\vartheta_3 = \sup(c_3 - 1/(2\theta J)), \quad \vartheta_5 = \sup(c_5 + f/J - \theta/(2J)) \quad (50)$$

As the right side of (49) is a negative definite function of the state vector (z_3, z_4, z_5, z_6) , the closed-loop system is globally asymptotically stable [8]. The result thus established is more precisely formulated in the following proposition:

Proposition 4 (Speed regulation). *Consider the closed-loop system composed of the induction machine, described by model (5), and the nonlinear controller defined by the control law (46). Then, one has the following properties:*

1) *The closed-loop error system undergoes, in the (z_3, z_4, z_5, z_6) coordinates, the following equations:*

$$\dot{z}_3 = -c_3 z_3 + z_5 / J + \tilde{\zeta}_3(z_3, z_5, \tilde{J} / J, \tilde{T}_L / J, \tilde{f} / J) \quad (51a)$$

$$\dot{z}_4 = -c_4 z_4 + z_6 \quad (51b)$$

$$\dot{z}_5 = -(c_5 + f/J) z_5 + \tilde{\zeta}_5(z_3, z_5, \tilde{J} / J, \tilde{T}_L / J, \tilde{f} / J) \quad (51c)$$

$$\dot{z}_6 = -c_6 z_6 - z_4 \quad (51d)$$

where

$$\tilde{\zeta}_3(z_3, z_5, \frac{\tilde{J}}{J}, \frac{\tilde{T}_L}{J}, \frac{\tilde{f}}{J}) \stackrel{\text{def}}{=} \frac{\tilde{J}}{J}(c_3 z_3 + \dot{\Omega}_{ref}) + \frac{\tilde{T}_L}{J} + \frac{\tilde{f}}{J}(\Omega_{ref} - z_3) \quad (51e)$$

$$\tilde{\zeta}_5(z_3, z_5, \frac{\tilde{J}}{J}, \frac{\tilde{T}_L}{J}, \frac{\tilde{f}}{J}) \stackrel{\text{def}}{=} \frac{\tilde{J}}{J}[(c_3 \hat{J} - \hat{f})(c_3 z_3 + \dot{\Omega}_{ref}) - c_3 z_5] + (c_3 \hat{J} - \hat{f}) \frac{\tilde{T}_L}{J} + \frac{\tilde{f}}{J}[(c_3 \hat{J} - \hat{f})x_3 + z_5] \quad (51f)$$

2) The above linear system is globally asymptotically stable with respect to the Lyapunov function V_4 .

Consequently, the errors (z_3, z_4, z_5, z_6) vanish exponentially fast, whatever the initial conditions \square

Remark 1. Note that the exponential nature of stability guarantees stability robustness with respect to modelling and measurements errors [8].

3.4 PFC Achievement

In the following proposition, it is shown that, for a specific class of reference signals, including periodic signals, the control objectives are achieved (in the mean) with an accuracy that depends, among others, on the network frequency ω_e . The following notations are needed to formulate results:

$$Z_1 = [z_1 \quad z_2 \quad k]^T; \quad Z_2 = [z_3 \quad z_4 \quad z_5 \quad z_6]^T, \quad \Delta = [\tilde{J}/J \quad \tilde{T}_L/J \quad \tilde{f}/J]^T \quad (52a)$$

$$a_0 = E^2/C; \quad a_1 = c_2 d C/E^2; \quad a_2 = \sqrt{2}E/C; \quad a_3 = d/E^2; \quad \varepsilon = 1/\omega_e \quad (52b)$$

$$A = \begin{pmatrix} A_1 & O_{(3,4)} \\ O_{(4,3)} & A_2 \end{pmatrix} \in \mathbb{R}^{7 \times 7} \quad (52c)$$

$$A_1 = \begin{pmatrix} -c_1 & 0 & 0 \\ 0 & 0 & a_0 \\ 0 & -a_1 & -d \end{pmatrix}; \quad A_2 = \begin{pmatrix} -c_3 & 0 & 1/J & 0 \\ 0 & -c_4 & 0 & 1 \\ 0 & 0 & -(c_5 + f/J) & 0 \\ 0 & -1 & 0 & -c_6 \end{pmatrix} \quad (52d)$$

$O_{(3,4)}, O_{(4,3)}$ null matrices in $\mathbb{R}^{3 \times 4}$ and $\mathbb{R}^{4 \times 3}$, respectively.

$$f(Z, t) = [0 \quad (a_0 k \cos(2\omega_e t) + a_2 z_1 \cos(\omega_e t)) \quad 0 \quad 0 \quad 0 \quad 0 \quad 0]^T \in \mathbb{R}^7 \quad (52e)$$

$$g = [0 \quad -1/C \quad a_3 \quad 0 \quad 0 \quad 0 \quad 0]^T \in \mathbb{R}^7 \quad (52f)$$

$$h_1 = [0 \quad 1 \quad -d C/E^2 \quad 0 \quad 0 \quad 0 \quad 0]^T \in \mathbb{R}^7 \quad (52g)$$

$$h_2(Z_2, \Delta) = [0 \quad 0 \quad 0 \quad \tilde{\zeta}_3(Z_2, \Delta) \quad 0 \quad \tilde{\zeta}_5(Z_2, \Delta) \quad 0]^T \quad (52h)$$

Proposition 5. Consider the system including the AC/DC/AC power converters and the induction motor, connected in tandem as shown in Fig.1. For control design purpose, the system is represented by its average model (6a-e). The system is set in closed-loop with the adaptive controller defined by the control laws (10, 18, 46) and the parameter adaptive law (44), where all design parameters (i.e.

$c_1, c_2, c_3, c_4, c_5, c_6, d$) are positive. Let the reference signals v_{dcref} , Ω_{ref} and Φ_{ref} be selected such that $v_{dcref} > 0$, $\Omega_{ref} \geq 0$ and Φ_{ref} equal to its nominal value. Then, one has the following properties:

1) The resulting closed-loop system undergoes the state-space equation:

$$\dot{Z} = A Z + f(Z, t) + g \rho(Z_2, t) + h_1 \dot{y}_{ref} + h_2(Z_2, \Delta) \quad (53)$$

2) Let the v_{dcref} , and Ω_{ref} be either constant or periodic signals, with period $N\pi / \omega_e$ (for some positive integer N), and suppose them to be time derivable (up to second order for Ω_{ref}) with bounded derivatives. Then, there exists a positive real ε^* such that, if $0 < \varepsilon < \varepsilon^*$ then:

a) The tracking error $z_2 = y - y_{ref}$ and the tuning parameter k are harmonic signals continuously depending on ε .

b) Furthermore,

$$i) \lim_{\varepsilon \rightarrow 0} z_2(t, \varepsilon) = 0; \quad ii) \lim_{\varepsilon \rightarrow 0} k(t, \varepsilon) = \bar{\rho}(0_4) / (a_0 C) \quad (54)$$

where $\bar{\rho}(0_4)$ denotes the mean value of the periodic time function $\rho(0_4, t)$ and 0_4 denotes the null vector of \mathbb{R}^4 \square

Remarks 2. a) The motor speed and the rotor flux norm both converge to their respective references because the errors (z_3, z_5) converge to zero as a result of Proposition 4.

b) Using Proposition 1 and the fact that the tuning parameter and its time derivative are available, we **get** that the error $z_1 = x_1 - x_1^* = i_e - k v_e$ converges exponentially fast to zero. The importance of Proposition 5 (part 2) lies (partly) in the fact that the (time varying) parameter k does converge to a fixed value (up to a harmonic error that depends on ω_e). This demonstrates that the PFC requirement is actually fulfilled with an accuracy that depends on ω_e . The **larger** ω_e , **the more** accurate the PFC quality. It will be seen in the next simulation study that the usual value $\omega_e = 50 \text{ Hz}$ leads to a quite acceptable quality.

c) Proposition 5 (Part 2) also demonstrates **that the tracking** objective is achieved (in the mean) for the DC-link squared voltage $y = x_2^2 = v_{dc}^2$ with an accuracy that depends on the voltage network frequency ω_e . The class of admissible references v_{dcref} and Ω_{ref} includes periodic signals with **the** period $N\pi / \omega_e$. That is, these signals must vary slower than the network voltage.

d) The fact that the tracking error $z_2 = v_{dc}^2 - v_{dcref}^2$ is harmonic proves the existence of output ripples. Proposition 5 (Part 2) ensures that the effect of ripples **is not significant** if ω_e is sufficiently large. It will be observed through simulations that the value $\omega_e = 50 \text{ Hz}$ leads to sufficiently small ripples. \square

4. SIMULATION

4.1 Simulation Protocol

The nonlinear adaptive controller, developed in Section 3, including the control laws (10, 18, 46) and the parameter adaptive law (42-44), **is now** evaluated by simulation. The simulated system is given the following **characteristics, corresponding** to a real-life experimental set-up available in the GIPSA Lab (Grenoble, France):

. Supply network: $v_e(t) = \sqrt{2} \cdot E \cos(\omega_e t)$ a single phase 220V/50Hz . AC/DC/AC converters: $L_1 = 15\text{mH}$; $C = 1.5\text{mF}$; modulation frequency 10 KHz . Induction machine: it is a 7.5KW motor whose characteristics are summarized in Table I. The indicated values of design parameters $c_1 = 10000$, $c_2 = 40$, $c_3 = 300$, $c_4 = 500$, $c_5 = 2 \times 10^5$, $c_6 = 900$, $d = 100$ have been selected using a ‘try-and-error’ search method and proved to be suitable.

CHARACTERISTICS	SYMBOL	VALUE	UNITY
Nominal power	P_n	7.5	kW
Nominal voltage	U_{sn}	380	V
Nominal flux	Φ_{rn}	1	Wb
Stator resistance	R_s	0.6	Ω
Rotor resistance	R_r	0.5	Ω
Number of pole pairs	p	2	
stator self inductance	L_s	98.3	Hm
rotor self inductance	L_r	90	Hm
Mutual inductance between the stator and rotor windings.	M_{sr}	90	mH

The simulation protocol is described by Figs. 2 to 4 which show that the reference signals and machine **load are** profiled so that the machine is enforced to operate, successively, both at high and low speeds and in motor and generator modes.

The DC-link voltage reference is set to the constant value $v_{dcref} = 600 \text{ V}$. The reference value Φ_{ref} for the rotor flux norm is set to its nominal value (1Wb).

Fig. 4 shows the changing inertia moment J and viscous friction coefficient f . The variations are 100% of the corresponding nominal values, approaching the physically allowed limits. The nonlinear controller developed in Section 3 will be applied.

4.2. Control performances in absence of model uncertainties

The controller performances are illustrated by Figs 3 and 5 to 8. Fig. 6 shows that the DC-link voltage $x_2 = v_{dc}$ is well regulated and quickly settles down after each change in the speed reference or the load torque. As expected by Proposition 5 and commented on in Remark 2c, the DC link voltage v_{dc} is subject to small amplitude ripples oscillating at the supply network frequency ω_e . The resulting input current i_e is illustrated by Fig 7. It is seen that the current amplitude changes whenever the speed reference or load torque vary (Fig. 2). However, the current frequency is insensitive to these changes. Specifically, the current remains (almost) always in phase or in opposed phase with the supply net voltage complying with the PFC requirement. This is further demonstrated by Fig. 5 which shows that the ratio k takes a constant value after transient periods following the changes in speed reference and load torque. The ratio k is negative whenever the network gets back some energy. This confirms Proposition 5 (part 2) and Remark 2c. Figs 2 and 8 show that the motor speed and the rotor flux norm match well their respective references (no ripples) despite the variation of mechanical parameters (load torque T_L , moment of inertia J and viscous friction coefficient f). This confirms the result of Proposition 4 and Remark 2a. For both controlled variables (Ω , Φ_r), the tracking quality is quite satisfactory at high speed as well as at low speed. The response time, after each change in speed reference and load torque, is less than 0.1 s. In this respect, let us note that the global convergence nature of the tracking results in Propositions 4 and 5 guarantee that all transients remain of finite duration, whatever the variable initial conditions and the unknown parameter jumps. Nevertheless, it is recommended to use any available prior knowledge to improve the choice of initial conditions in control laws and in parameter adaptive laws.

4.3. Control performances in presence of errors on model nominal parameters

The robustness of the proposed control to modeling errors is now illustrated by considering errors on the nominal values of some parameters. The parameters R_r , R_s , L_s , L_r , and M_{sr} are given a different value higher than 50% compared to the true system model parameters. Specifically, the (unknown) true system parameters are used in the simulated machine model while the nominal values are used in the control laws (46-47). The experimental operation protocol is kept unchanged with respect to Subsection 4.2. The obtained control scheme's performances are illustrated by Fig 9 where the tracking errors for both rotor flux and rotor speed are plotted. For comparison purpose, the tracking errors obtained in the case of no difference between the simulator and controller parameters (i.e. nominal parameters equal true parameters) are also plotted in Fig. 9. It is seen clearly seen that the tracking errors obtained when the nominal parameters deviate from the true parameters remain quite

close to those obtained in the parameters coincide. In both cases, the rotor flux norm and rotor speed match well their references and converge to them after a transient period of nearly 0.02s.

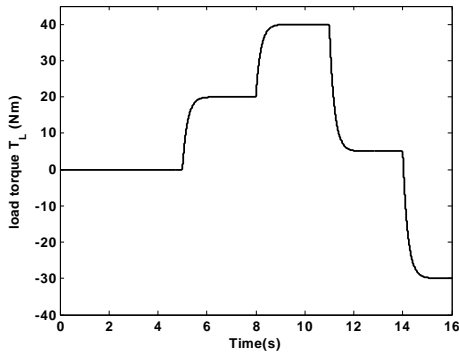


Fig. 2. Applied load torque

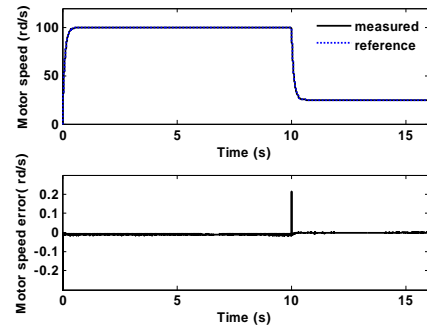


Fig. 3. Rotor speed Ω (rd/s) . Upper: reference and measured speed; lower: speed error control.

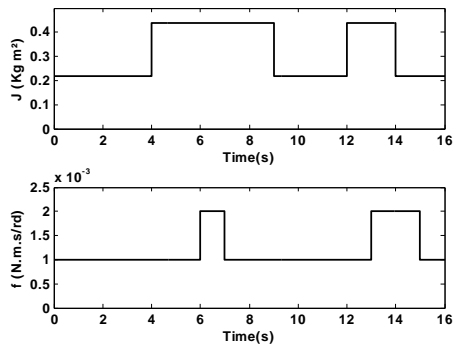


Fig. 4. Upper: Rotor inertia variation. lower: Friction coefficient variation

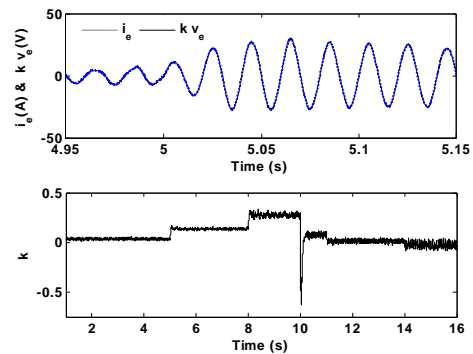


Fig. 5. Upper: Reference and measured AC-link current i_e (A). lower: Tuning parameter k

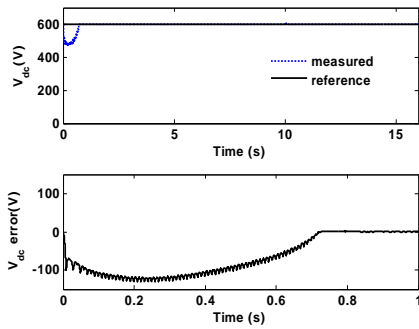


Fig. 6. DC-link voltage v_{dc} (V) . Upper: reference and measured; lower: error control

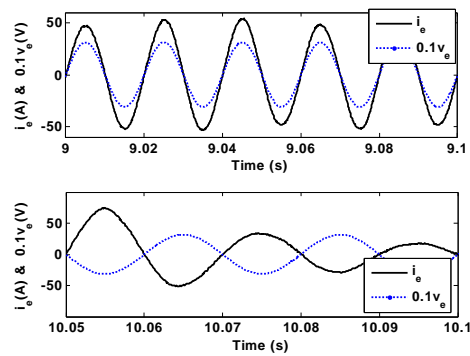


Fig. 7. Unitary power factor checking in presence of a varying speed reference and load torque,

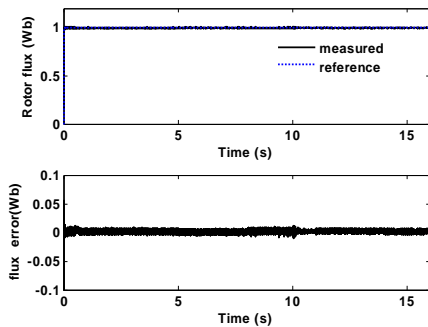


Fig. 8. Rotor flux norm (Wb) response. Upper: reference and measured; lower: error control

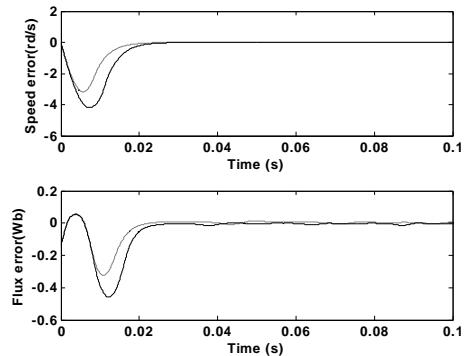


Fig. 9. Control performances in presence of parameter bias. Upper: speed tracking error. Lower: rotor flux norm tracking error.

5. CONCLUSION

The problem of controlling associations including AC/DC rectifier, DC/AC inverter and induction motor has been addressed. The system dynamics have been described by the averaged seventh order nonlinear state-space model (6a-g). Based on such a model, the multi-loops nonlinear adaptive controller defined by (10, 18, 42, 43, 44, 46) has been designed and analyzed using tools from the Lyapunov stability and averaging theory. It was formally established that the proposed controller achieves the objectives it has been designed for, i.e. (i) an almost unitary power factor; (ii) a tight regulation of DC-link voltage (v_{dc}); (iii) a satisfactory rotor speed reference tracking over a wide range of mechanical parameter variations; (iv) a tight regulation of the rotor flux norm. These results have been confirmed by a simulation study which further showed additional features of the proposed controller, e.g. its weak sensitivity to electrical model parameters, its supremacy over conventional regulators. To the authors' knowledge, it is the first time that a so complete formal control design and analysis framework is developed for induction motors and associated power converters.

APPENDIX : Proof of proposition 5

Proof. Part 1. Substituting the right sides of (46) to u_2 and u_3 in (13) leads to:

$$\chi(x, t) = -\rho(Z_2, t) / C \quad (55)$$

where we have used (52a-g). Substituting the right side of (55) to $\chi(x, t)$ in (19) gives:

$$\dot{Z}_1 = A_1 Z_1 + \left(\frac{\rho(Z_2, t)}{C} + \dot{y}_{ref} \right) \begin{pmatrix} 0 \\ -1 \\ d C / E^2 \end{pmatrix} + \begin{pmatrix} 0 \\ \frac{E^2}{C} k \cos(2\omega_e t) + \frac{\sqrt{2}}{C} E z_1 \cos(\omega_e t) \\ 0 \end{pmatrix} \quad (56)$$

where notations (52b-g) have been used. Putting together (56) and (51) in a global state space equation one gets (53) and proves Part 1.

Part 2. As v_{dcref} , and Ω_{ref} as well as their derivatives are constant or periodic (with period $N\pi/\omega_e$), it follows that the system (53) is periodically time-varying. Therefore, the averaging theory turns out to be a suitable framework to analyze its stability (see e.g. [8]). To this end, introduce the time-scale change $\tau = \omega_e t$ and the following signal changes:

$$W(\tau) = Z(t), \quad y_{ref}^*(t) = y_{ref}(Nt/2\omega_e), \quad \Omega_{ref}^*(t) = \Omega_{ref}(Nt/2\omega_e) \quad (57a)$$

This readily implies that y_{ref}^* , and Ω_{ref}^* are in turn constant or periodic, with period 2π , and:

$$y_{ref}^*(t) = y_{ref}^*(2\tau/N), \quad \Omega_{ref}^*(t) = \Omega_{ref}^*(2\tau/N). \quad (57b)$$

Also, it is easily seen that $\dot{W}(\tau) = dW(\tau)/d\tau = \varepsilon dZ(t)/dt = \varepsilon \dot{Z}(t)$ with $\varepsilon = 1/\omega_e$. Then, it follows from (53) and using (57b), that the state vector W undergoes the following state equation:

$$\dot{W} = \varepsilon A W + \varepsilon f_1(W, \tau, \varepsilon) + \varepsilon g \rho_1(W_2, \tau, \varepsilon) + h_1 \dot{y}_{ref}^* (2\tau / N) + h_2(W_2, \Delta) \quad (58a)$$

with

$$f_1(W, \tau, \varepsilon) = f(W, \varepsilon\tau), \quad \rho_1(W_2, \tau, \varepsilon) = \rho(W_2, \varepsilon\tau) \quad (58b)$$

It readily follows from (52e) that:

$$f_1(W, \tau, \varepsilon) = [0 \quad (a_0 k \cos(2\tau) + a_2 w_1 \cos(\tau)) \quad 0 \quad 0 \quad 0 \quad 0 \quad 0]^T \quad (58c)$$

where the following notations are adopted in coherence with (52a):

$$W = [W_1^T \quad W_2^T]^T, \quad W_1 = [w_1 \quad w_2 \quad w]^T, \quad W_2 = [w_3 \quad w_4 \quad w_5 \quad w_6]^T \quad (59)$$

According to the system averaging theory, one gets stability results regarding the system of interest (58a-b) by analyzing the averaged system defined by:

$$\overline{\dot{W}} = \varepsilon A \overline{W} + \varepsilon \overline{f_1}(\overline{W}) + \varepsilon g \overline{\rho_1}(\overline{W}_2) + \overline{h_2}(\overline{W}_2, \Delta) \quad \text{where } \overline{W} \in \mathbb{R}^7 \quad (60a)$$

with

$$\overline{f_1}(\overline{W}) = \lim_{\varepsilon \rightarrow 0} \frac{1}{2\pi N} \int_0^{2\pi N} f_1(\overline{W}, \tau, \varepsilon) d\tau, \quad (60b)$$

$$\overline{\rho_1}(\overline{W}_2) = \lim_{\varepsilon \rightarrow 0} \frac{1}{2\pi N} \int_0^{2\pi N} \rho_1(\overline{W}_2, \tau, \varepsilon) d\tau \quad (60c)$$

$$\overline{h_2}(\overline{W}_2, \Delta) = \lim_{\varepsilon \rightarrow 0} \frac{1}{2\pi N} \int_0^{2\pi N} h_2(\overline{W}_2, \Delta, \tau, \varepsilon) d\tau \quad (60d)$$

Note that the last term on the right side of (58a) has not been accounted for in (60a) because its average value is null, due to the periodicity (with period 2π) of y_{ref}^* . From (58c), one has:

$$\overline{f_1}(\overline{W}) = [0 \quad 0 \quad 0 \quad 0 \quad 0 \quad 0 \quad 0]^T \quad (61)$$

In view of (61) the average system (60a) simplifies to:

$$\overline{\dot{W}} = \varepsilon A \overline{W} + \varepsilon g \overline{\rho_1}(\overline{W}_2) + \overline{h_2}(\overline{W}_2, \Delta) \quad (62)$$

where the following notations are used in coherence with (59) and (60a):

$$\overline{W} = [\overline{W}_1^T \quad \overline{W}_2^T]^T, \quad \overline{W}_1 = [\overline{w}_1 \quad \overline{w}_2 \quad \overline{w}]^T, \quad \overline{W}_2 = [\overline{w}_3 \quad \overline{w}_4 \quad \overline{w}_5 \quad \overline{w}_6]^T \quad (63)$$

In view of (52f), the vector g assumes the following partition:

$$g = [g_1^T \quad 0_4^T]^T \quad \text{with } g_1 = [0 \quad -1/C \quad a_3]^T, \quad 0_4 = [0 \quad 0 \quad 0 \quad 0]^T \quad (64)$$

This together with (52d) implies that (60a) can be decomposed in the following two state equations:

$$\overline{\dot{W}}_1 = \varepsilon A_1 \overline{W}_1 + \varepsilon g_1 \overline{\rho_1}(\overline{W}_2) \quad (65a)$$

$$\overline{\dot{W}}_2 = \varepsilon A_2 \overline{W}_2 + \overline{h_2}(\overline{W}_2, \Delta) \quad (65b)$$

It has already noted (see Proposition 4) that if c_3, c_4, c_5, c_6 are positive. Then, it follows from (65b) that:

$$\lim_{t \rightarrow \infty} \overline{W}_2(t) = 0_4 \quad (66)$$

exponentially and whatever $\overline{W}_2(0)$. Then:

$$\lim_{t \rightarrow \infty} \overline{\rho}_1(\overline{W}_2(t)) = \overline{\rho}_1(0_4) \quad (67)$$

exponentially and whatever $\overline{W}_2(0)$. Now, let us check that A_1 is in turn Hurwitz. Its characteristic polynomial is:

$$\det(\lambda I - A_1) = \lambda^3 + (c_1 + d)\lambda^2 + d(c_1 + c_2)\lambda + d c_1 c_2 \quad (68)$$

Applying for instance the well known Routh's algebraic criteria, it follows that all zeros of the polynomial (68) have negative real parts if the coefficients (c_1, c_2, d) are positive which **is actually** the case. Hence, the matrix A_1 is **Hurwitz, implying** that the autonomous part of the linear system (65a) is globally exponentially stable. Then, one gets from (66) that the solution of the nonautonomous system (65a) satisfies:

$$\lim_{t \rightarrow \infty} \overline{W}_1(t) = -\overline{\rho}_1(0_4) A_1^{-1} g_1 \quad (69)$$

exponentially and whatever $\overline{W}_1(0)$. Again, the exponential feature of the convergence is due to the linearity of (65a). Combining (66) and (69), it follows that the state vector

$$W^* \stackrel{\text{def}}{=} \begin{bmatrix} -\overline{\rho}_1(0_4) A_1^{-1} g_1 \\ 0_4 \end{bmatrix} \in \mathbb{R}^7 \quad (70)$$

is a globally exponentially stable equilibrium of the average system (62). Now, invoking **the** averaging theory (e.g. Theorem 10.4 in [8]), we conclude that there exists a positive real constants ε^* such that, for all $0 < \varepsilon < \varepsilon^*$, the differential equation (58a) has a 2π -periodic solution $W(\tau) = W(\tau, \varepsilon)$, that continuously depends on ε and that:

$$\lim_{\varepsilon \rightarrow 0} W(\tau, \varepsilon) = W^* \quad (71a)$$

The same result applies to the differential equation (56) using the relation $Z(t) = W(\tau)$ with $\tau = \omega_e t$. That is, $Z(t) = Z(t, \varepsilon)$ is $(2\pi / \omega_e)$ -periodic, it depends continuously on ε and:

$$\lim_{\varepsilon \rightarrow 0} Z(t, \varepsilon) = W^* \quad (71b)$$

This establishes Part 2-a of Proposition 5.

To prove Part 2-b, let us obtain more insight on the equilibrium W^* . In coherence with (52a), this is decomposed as follows:

$$W^* = \begin{bmatrix} W_1^{*T} & W_2^{*T} \end{bmatrix}^T, \quad W_1^* = \begin{bmatrix} w_1^* & w_2^* & w^* \end{bmatrix}^T, \quad W_2^* = \begin{bmatrix} w_3^* & w_4^* & w_5^* & w_6^* \end{bmatrix}^T \quad (72)$$

Then, it readily follows from (70) that:

$$W_1^* = -\bar{\rho}_1(0_4)A_1^{-1}g_1 \quad \text{and} \quad W_2^* = 0_4 \quad (73)$$

Also, it is readily checked using (52d) and (64) that:

$$W_1^* = -\bar{\rho}_1(0_4)A_1^{-1}g_1 = -\bar{\rho}_1(0_4) \begin{bmatrix} 0 & (d - Ca_0a_3)/(Ca_0a_1) & -1/(Ca_0) \end{bmatrix}^T \quad (74)$$

one gets from (52b), (71b), (72), (74) and (75) that:

$$\lim_{\varepsilon \rightarrow 0} z_2(t, \varepsilon) = w_2^* = 0 \quad (76a)$$

$$\lim_{\varepsilon \rightarrow 0} k(t, \varepsilon) = w^* = \bar{\rho}_1(0_4)/(Ca_0) \quad (76b)$$

Finally, notice that:

$$\begin{aligned} \bar{\rho}_1(0_4) &= \lim_{\varepsilon \rightarrow 0} \frac{1}{2\pi N} \int_0^{2\pi N} \bar{\rho}_1(0_4, \tau, \varepsilon) d\tau \quad (\text{using (60c)}) \\ &= \lim_{\varepsilon \rightarrow 0} \frac{1}{2\pi N} \int_0^{2\pi N} \rho(0_4, \varepsilon\tau) d\tau \quad (\text{using (58b)}) \end{aligned} \quad (77a)$$

Introducing the variable change $\tau = \omega_e t$, (69a) becomes:

$$\bar{\rho}_1(0_4) = \lim_{\varepsilon \rightarrow 0} \frac{\omega_e}{2\pi N} \int_0^{2\pi N/\omega_e} \rho(0_4, t) dt = \bar{\rho}(0_4) \quad (77b)$$

This, together with (76a-b), establishes Part 2-b and completes the proof of Proposition 5 ■

Table II. Main notations

c_i, d :	design parameters	x_3 :	(average) rotor speed ($x_3 = \bar{\Omega}$)
f_e	voltage network frequency (Hz)	x_4 :	(average) α -axis stator current ($x_4 = \bar{i}_{s\alpha}$)
$i_{s\alpha}, i_{s\beta}$:	α - and β - axis stator currents	x_5 :	(average) β -axis stator current ($x_5 = \bar{i}_{s\beta}$)
i_e :	rectifier input current	x_6 :	(average) α -axis rotor flux ($x_6 = \bar{\phi}_{r\alpha}$)
$L_1, 2C$:	passive components of input converter	x_7 :	(average) β -axis rotor flux ($x_7 = \bar{\phi}_{r\beta}$)
$s \in \{-1, 1\}$:	PWM input signal controlling converter IGBT's	y :	(average) squared DC Link voltage $y = x_2^2 = \bar{v}_{dc}^2$
T_L :	machine load torque	y_{ref} :	reference value of y i.e. $y_{ref} = v_{dcref}^2$
$u_{i=1,2,3}$:	duty ratios i.e. average values of s and the three phase duty ratio system (s_1, s_2, s_3) over cutting periods	z_1 :	input current tracking error $z_1 = x_1 - kv_e$
$v_{s\alpha}, v_{s\beta}$:	α - and β - axis stator voltages	z_2 :	squared DC Link voltage error $z_2 = y - y_{ref}$
v_{dc} :	rectifier output voltage	z_3 :	rotor speed tracking error $z_3 = \Omega_{ref} - \bar{\Omega}$
v_{dcref} :	reference value of rectifier output voltage v_{dc}	z_4 :	rotor flux norm tracking error $z_4 = \Phi_{ref}^2 - \Phi_r^2$
$v_e(t)$:	AC line voltage	z_5, z_6 :	additional error variables in control design
V_i :	Lyapunov functions introduced in various control design steps ($i = 1 \dots 6$)	Φ_r	rotor flux norm $\Phi_r = \sqrt{(x_6^2 + x_7^2)}$
x_1^* :	input current reference $x_1^* = kv_e$	Ω_{ref} :	reference value of machine rotor angular velocity
x_2 :	(average) rectifier output voltage $x_2 = \bar{v}_{dc}$	ε :	inverse of supply net frequency i.e. $\varepsilon = 1/\omega_e$

REFERENCES

- [1] Duarte-Mermoud M. A., J. C. Travieso-Torres, I. S. Pelissier, H. A. González. "Induction motor control based on adaptive passivity", *Asian Journal of Control*, Vol. 14, No. 2, pp. 1- 18, (2012).
- [2]. Ryan M.J., R.D. Lorenz, R.W. De Doncker. "Modeling of Sinewave Inverters: A Geometric Approach". Industrial Electronics Society, 1998. IECON '98. Proceedings of the 24th Annual Conference of the IEEE, Aachen, Germany, (1998).
- [3] Barambones. O, P. Alkorta. "Vector Control for Induction Motor Drives Based on Adaptive Variable Structure Control Algorithm", *Asian Journal of Control*, Vol. 12, No. 5, pp. 640- 649, (2010).
- [4] Marques G.D. "A PWM Rectifier Control System with DC Current Control Based on the Space Vector Modulation and Stabization", *Seventh International Conference on Power Electronics and Variable Speed Drives*, London, UK, (1998).
- [5]. Ortega R., P.J. Nicklasson , G. Espinosa-Perez. "On Speed Control of Induction Motors", *Automatica*, Vol 32, no 3, pp 455-460, (1996).
- [6] Sira H., R. Silva. "Control Design Techniques in Power Electronics Devices". Springer, (2006).
- [7] Singh B., G. Bhuvaneswari, V. Garg. "Improved Power Quality AC-DC Converter for Electric Multiple Units in Electric Traction". *IEEE Power India Conference*, New Delhi, (2006).
- [8] Khalil H., "Nonlinear systems". Prentice Hall, (2003).
- [9] Krstic M., I. Kanellakopoulos, P. Kokotovic "Nonlinear and Adaptive Control Design". John Wilay & Sons, Inc. (1995).
- [10] Traoré D., F. Plestan, A. Glumineau, J. DE Leon. "Sensorless Induction Motor: High Order Sliding Mode Controller and Adaptive Interconnected Observer", *IEEE Transactions on Industrial Electronics*, Vol. 55, no.11, pp 3818- 3827, (2008).
- [11] Jasinski M., M. Cichowlas, M. P. Kazmierkowski. "Direct Control for AC/DC/AC Converter-Fed Induction Motor With Active Filtering Function", *The International Journal for Computation and Mathematics in Electrical and Electronic Engineering*, Vol. 25, no. 1. pp. 235-242, (2006).
- [12] Xiong Jian, Kang Yong, Duan Shan Xu, Zhang Kai, Chen Jian."Simplified Control Circuit of Three Phase PWM Rectifier", *IEEE Applied Power Electronics Conference and Exposition, APEC '99. 4th Annual*, Dallas. TX. USA, (1999).